JOURNAL OF MATERIALS SCIENCE 7 (1972) 1197–1215

Review: on the structure and microstructure of quenched beta-brass type alloys

L. DELAEY
Department of Metallurgy, Katolieke Universiteit Leuven, Belgium

A. J. PERKINS*, T. B. MASSALSKI
Metal Physics Laboratory, Center for Special Studies, Mellon Institute of Science, Carnegie-Mellon University, Pittsburgh, Pennsylvania, USA

Quenched beta-phase alloys in systems based on the noble metals are often thermodynamically metastable. A review of the information derived from transmission electron microscopy indicates the presence of various anomalous contrast and diffraction effects in such alloys. Contrast effects may be referred to as mottling, striation, cross-hatching, etc., and they may change in intensity with respect to different extinction contours, foil thickness and foil tilting. Diffraction effects refer to diffuse streaking in certain directions, the appearance of additional maxima or their splitting, and slight deviations from cubic symmetry. The possible causes for the presence of such features are discussed in the present paper. Some effects are considered to be at least in part the result of surface rippling, caused by electropolishing, but other effects are associated with the presence of precipitates, or with atomic displacements from ideal bcc packing. A detailed analysis of the diffraction effects suggests that structural features must be present analogous to the hexagonal ω-phase (known in transition alloys), and the nearly hexagonal α' phase (known in bainitic structures). The stability of the beta-phase alloys is considered in terms of the above features, concluding that both vibrational and electronic entropy terms may be contributing, and that instability at low temperatures may be manifested in a number of ways not all of which fit into conventional phase-transformation categories.

1. Introduction

The metastable beta-phases of noble-metal alloy systems may transform in a number of ways. These involve both diffusional and diffusionless transformation modes, including martensitic, bainitic, and massive reactions. All of these modes have been studied in detail by various previous workers; martensitic transformations in noble-metal alloys have been recently reviewed by Warlimont and Delaey [1]; the work on nonferrous bainites has been summarized most recently by Hehemann [2], Clark and Wayman [3], and Garwood [4]; massive transformations in supersaturated beta-phases have been treated in the work of Massalski and co-workers which also has been recently reviewed [5].

In all of these various investigations of transformations of bcc phases, it has been assumed that the parent phase has a simple bcc, CsCl or Fe_3Al structure. However, the use of transmission electron microscopy in the more recent studies has revealed a possible substructure existing within the supersaturated parent beta-phases of various alloys. These observations have usually been made on retained beta-phases in quenched alloys, and generally take the form of anomalous contrast and diffraction effects. These features have been reported or commented on only briefly by numerous authors whose prime concern was one of the well-known beta-phase transformation modes mentioned above [6-12]. A brief review of these

*Now at Naval Post Graduate School, Monterey, California USA.

observations will be made in the next section.

If it is true that the parent bcc phase is in some way abnormal, such as by containing fine precipitates, then the effect on other phase-transformation modes is likely to be significant. The presence of fine precipitates, for example, would be likely to have a pronounced effect on nucleation events and kinetics, such as for the case of martensite and massive type reactions. In addition, if the observed anomalous effects are due to some strain or distortion of the beta structure, then the effect on structures of developing martensites or bainites could be significant. For this reason, it was considered important to investigate in some detail the nature of a number of quenched, supersaturated beta-brass type phases, to ascertain the causes of the anomalous observations, and to be able to predict the effect of these phenomena in the matrix phase on the important transformation modes in these alloys.

2. Literature survey

Most of the observations of anomalous effects in beta-brass type alloys have been reported on alloys of the Cu-Zn systems. In various investigations of Cu-Zn alloys, transmission microstructures and diffraction data have been presented for the beta-phase accompanying martensitic [6, 7], bainitic [8-10], Widmanstätten [11], and massive [12] transformation products. In most cases the observations were incidental to the main theme of a particular study, and for the most part were only briefly mentioned, if at all. The presence of anomalous contrast and diffraction effects is obvious, however (though not always mentioned) in numerous published figures. An examination of these structures convinces one immediately that the general condition of the bcc phases is significantly disturbed.

The comments by Hawbolt and Massalski [12] in their observations of the beta-phase accompanying massive transformations in the Cu-Zn system, are of general interest: "The metastability of the quenched beta-phase may be of considerable importance in massive transformations produced following a rapid reheating of thin metastable product . . . if, as suggested by electron microscopy studies, the beta-phase is unstable at room temperature and a coherent precipitation does develop, then the . . . time required for dissolution of this precipitation product . . . would affect the growth of . . . any other effective nuclei." Similar thoughts could be, but have not been, applied to the effect of beta matrix conditions on bainitic and martensitic reactions. The remarks of Hornbogen and Warlimont [8] about the retained beta-phase associated with bainitic products are typical of several other Cu-Zn bainite studies: (translated from German) "The mottling in the matrix phase . . . indicates that a non-homogeneous metastable state remains after quenching of beta-brass to room-temperature. Many coherent precipitates form in the bcc lattice . . . ." No mention is made, in any of the accounts of investigations of Cu-Zn bainite or martensite, of the possible effect or relation of this instability in the bcc phase to other reactions in the alloys.

In addition to the published data on Cu-Zn alloys, similar beta-phase anomalies (published and unpublished) have been revealed in the course of investigations dealing with other noble-metal alloys, such as Cu-Sn [13-16], Cu-Be [16, 17], Cu-Al-Ni [18], Cu-Ga-Ge [19], and others. In the present investigation, the systems Ag-Cd, Ag-Zn, Cu-Zn-Ga, and Cu-Zn-Al are added to these. It should be pointed out immediately that in the case of Cu-Sn and Cu-Be alloys, it is now fairly clear that the observed beta-phase effects, although very similar to those in the other alloys, have a different fundamental origin, being due to precipitation of fine particles of the equilibrium delta phase in the case of Cu-Sn [14], and due to ordering in the case of Cu-Be [17].

The nature of the anomalous effects which have been reported can be summarized as follows: (i) in bright-field transmission images, the beta-phase appears "mottled", usually in some regular pattern (cross-hatched, striated or speckled); (ii) the contrast effects are maximized near extinction contours, and change drastically with orientation (foil tilting). Several reports give reason to believe that the mottling becomes more pronounced after low-temperature ageing of the beta-phase [10, 11]. The mottling is of a much finer scale than the domain size, and therefore does not appear to be generally related to ordering. The mottled effect is also often seen in supersaturated fcc phases (such as massive α_m), but disappears on annealing. In terms of diffraction, the general effects are: (i) diffuse streaking in certain directions, sometimes found to be complete {1 1 1} planes of intensity in reciprocal space; (ii) splitting of certain diffraction spots and the appearance of some extra maxima; (iii) slight deviation from cubic symmetry.

These microscopic observations and diffraction effects have been variously interpreted, usually on the basis of incomplete arguments. The following descriptions have been applied prematurely by various authors to explain the beta-phase anomalies in microscopy or diffraction, or both: (i) strain contrast around coherent precipitate particles [15]; (ii) fine precipitate particles surrounded by envelopes of rejected zinc [28]; (iii) coherent precipitates on {1 1 0} planes [12]; (iv) fine-scale strain-induced martensite [7]; (v) temperature-diffuse scattering [13]. The crystal structures of any possible precipitates or martensite have not been rigorously sought by any investigators.

Only a few studies have dealt more directly with the metastable state of quenched beta-phase alloys [10-15]. Hull [20], in an investigation concerned primarily with spontaneous martensite formation at the edges of Cu-Zn thin foils, touched on the accompanying mottled effect in the beta-matrix. His observations on the effect were restrained and brief, but ultimately more correct than most; Hull commented that the mottled appearance of the beta-phase foils seemed to be a result of electropolishing, and noted that spontaneous martensite formed in the same foils after polishing did not contain the mottled contrast. These remarks are the most perceptive and valuable to be found in the literature, and will be seen to be quite consistent with the results of the present study. A brief note by Warlimont [15] also dealt specifically with the anomalous effect in several alloys, including Cu-Zn and Cu-Sn, but only general remarks with respect to interpretation were offered.

3. Experimental

For the experimental portion of this study, use was made of alloys available from several previous investigations in our laboratories. Alloys from the systems Cu-Zn, Cu-Zn-Ga, Cu-Zn-Al, Ag-Cd and Ag-Zn were examined by transmission electron microscopy. All of these alloys were prepared from metals of 99.999% purity or better. In the general casting procedure, the weighed materials were contained in graphite crucibles and encapsulated in silica tubes which were evacuated with a mechanical pump, heated to bake out adsorbed water and back-filled with $\frac{1}{2}$ atm of helium. The alloys were held at approximately 150°C above their respective melting temperatures for $\frac{1}{2}$ h, and were shaken vigorously several times during this interval to assure complete mixing of the components. The tubes were then quenched into water. The ingots were re-encapsulated and homogenized by holding at a temperature high in the single-phase beta field for 48 h, then quenched into iced brine. The samples were carefully weighed before and after casting, and after homogenization, and in all cases were found to be within 0.04% of the initial weight.

Pieces less than 0.38 mm in thickness, suitable for thin-foil specimen preparation, were obtained from the ingots by either sawing and sanding out thin sections directly or by cold-rolling, followed by punching of 3 mm diameter discs. In the case of the cold-rolling procedure, intermediate anneals were necessary; time and temperature were minimized to prevent volatilization of alloying elements. The 3 mm discs were solution-treated in the beta-phase in all cases, then quenched at various rates. All of the specimens examined contained retained supersaturated beta-phase, often accompanied by a decomposition product such as massive or Widmanstätten alpha-phases. Foils for transmission electron microscopy were prepared by electropolishing by jet and window techniques; the solutions and conditions used were either: (i) 10% KCN solution in water, 10 to 20 volts ac, graphite electrode, room-temperature; or (ii) 2 to 1 methanol/HNO_3 solutions, 15 to 30 volts dc, stainless steel cathode, 0°C. Electron microscopy was performed using a Philips 200 EM equipped with a $\pm$ 30°C tilt, 360° rotation stage, and operated at 100 kV.

4. Results and discussion

4.1. General aspects of the contrast effect

Anomalous contrast effects were observed when studying the structure and microstructure of various quenched supersaturated beta-phases by means of transmission electron microscopy. The contrast changes drastically with crystal orientation and is at a maximum near the extinction contours belonging to the bcc phase. The effects are exemplified by the binary and ternary Cu-Zn beta-phases. Fig. 1 shows the typical mottled contrast effect in a Cu-Zn-Ga beta-phase where the orientation of the foil was close to $(0\,0\,1)_\beta$. The contrast effect in this case appears as short lines in two perpendicular directions. If the foil surface has another crystallographic orientation, the contrast changes in appearance, as seen in Fig. 2, where the foil orientation was close to $(1\,1\,1)_\beta$.

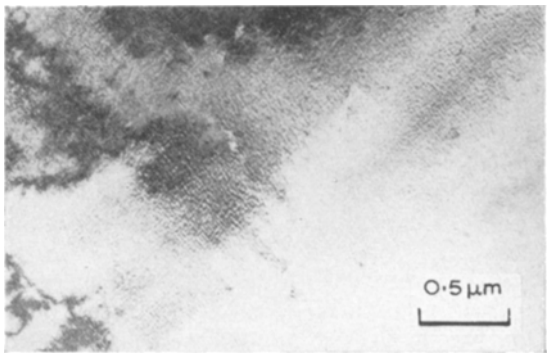

Figure 1 Typical mottled contrast in quenched supersaturated beta-phase of a Cu-Zn-Ga alloy; orientation of foil near $(001)_\beta$.

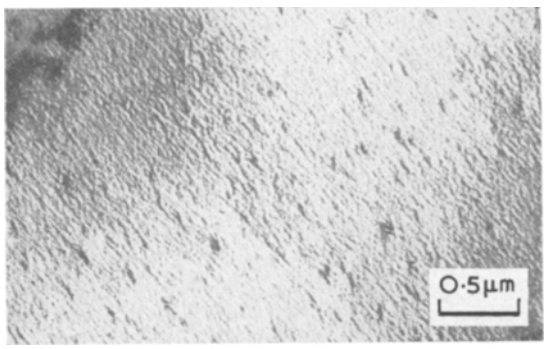

Figure 2 The same alloy as in Fig. 1. Orientation of foil near $(111)_\beta$ produces a change in the contrast compared with Fig. 1.

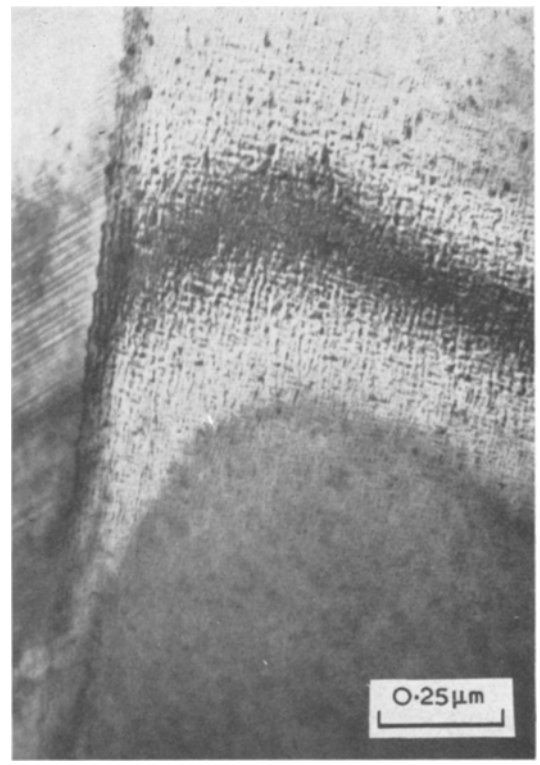

Figure 3 Contrast in a supersaturated Ag-44.0% Cd β-phase alloy. Strongest mottled contrast effect is close to the extinction contours.

The contrast effect becomes more pronounced in the supersaturated Ag-Cd beta-phases. Fig. 3 shows again that the contrast effect is strongest close to the extinction contours, whereas in areas far from the extinction contours, the contrast is weaker; however, in this case the visible contrast even away from contours has the appearance of very fine precipitates lying along two perpendicular directions; an enlargement of an area of Fig. 3 clearly shows this (Fig. 4).

More information about the distribution of the precipitates can be obtained if the contrast distribution visible in Fig. 4 is also analysed by means of an optical diffraction technique, using a laser beam. Fig. 5 shows that the precipitates lie preferentially along two perpendicular directions (this can be derived from the streaking). From the position of the maximum along those streaks, it can be shown that the particles are regularly distributed along the two directions, giving to the material a long-range periodicity. These conclusions from the optical diffractogram are clearly visible on Fig. 4 itself. The result obtained by optical diffraction shows the influence of morphological distribution on the fine structure of the diffraction spots. It indicates that the periodical arrangement of the precipitates in the β-matrix may cause some effects in the electron diffraction patterns. This method of analysing electron micrographs has not yet been perfected, but it is hoped that in the future electron micrographs of finely distributed particles may be studied by optical diffraction in order to separate the diffraction effects due to the content of the unit cell from those due to the distribution of the precipitates.

The massively formed α_m-phase which often form in these alloys are also supersaturated and show similar contrast effects to the β-phase. Figs. 6 and 7 show the mottled contrast in Cu-Zn and Ag-Cd α_m-phases, respectively. On pulse-heating the quenched β-phase, the equilibrium α-phase may form together with the massive α_m-

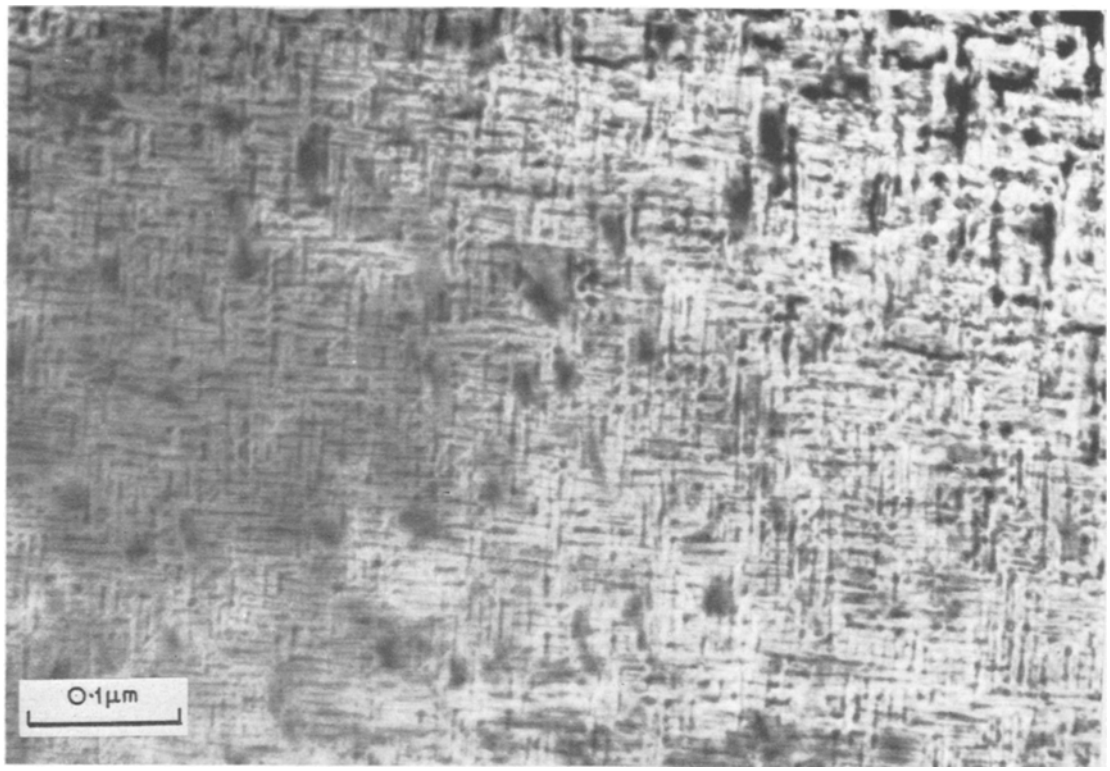

Figure 4 Enlargement of an area of Fig. 3 has the appearance of fine precipitates on two mutuàlly perpendicular planes.

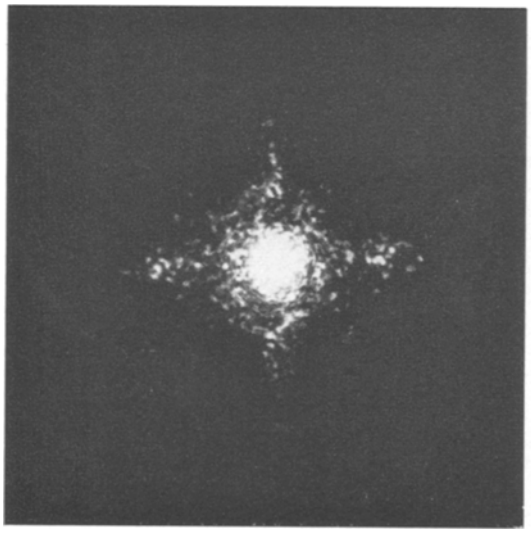

Figure 5 Contrast distribution of Fig. 4 analysed by means of optical diffraction using a laser beam. (Courtesy of Dr R. DeRidder and Professor S. Amelinckx.)

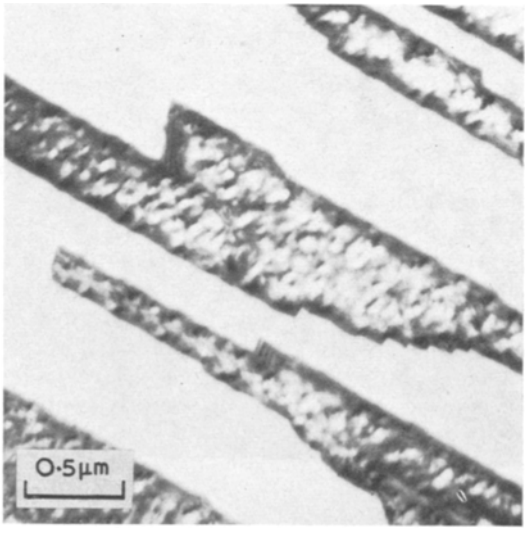

Figure 6 Contrast effects obtained in massive alpha (α_m) phases of the Cu-Zn system; only the twinned areas of the fcc phase are in contrast.

phase, as described by the recent work of Ayers and Massalski [21] in Ag-Zn alloys. In this case, the equilibrium α-phase forms by a diffusional process and usually takes a Widmanstätten

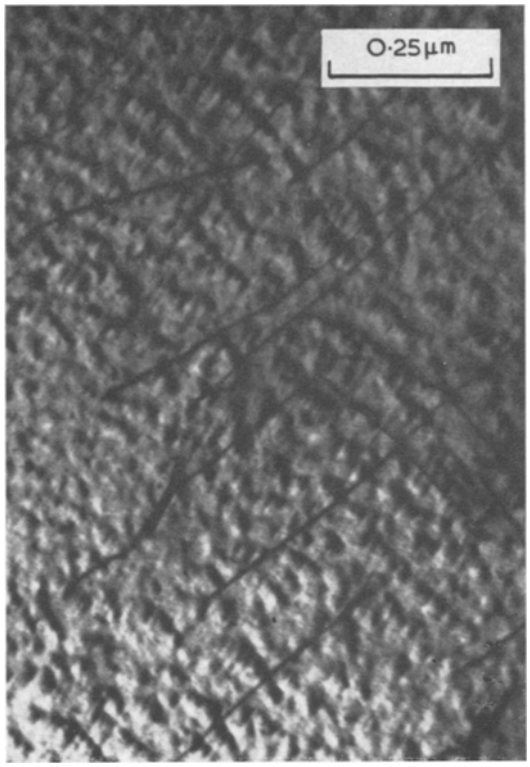

Figure 7 Mottled contrast seen in a Ag-44.0% Cd alloy containing α_m phase formed by rapid quenching from the β-phase field.

morphology (α_w) [21]. The α_w equilibrium phase shown in Fig. 8 after pulse-heating and quenching shows none of the mottled contrast effect shown above for massively-formed α_m grains; the surrounding phase in this region is retained supersaturated β-phase, which shows the usual contrast effect.

Fig. 9 shows an area in which a portion of a Cu-Zn β-phase has transformed into martensite upon quenching. The martensite, having an orientation close to the basal plane, shows no mottled contrast effect, whereas the retained supersaturated β-phase shows extensive mottling. In the middle of the figure the boundary between the β-phase and the martensite is evident; its projection through the foil thickness can be seen. This boundary exhibits an association of each of the dark parallel lines of the martensite with the mottling in the β-phase. This area showed that the β-phase contained thin platelets; no extra intensity maxima could be detected in the diffraction pattern taken from this region, however. Upon tilting the specimen, the contrast of the lines in the boundary changed continuously.

The fact that the mottling effect was absent in the martensite mentioned above should not be interpreted as meaning that mottling does not appear in any martensites of these β-phase alloys. In fact, mottling does appear in some martensitic β-brass alloys, and is typically visible only in the vicinity of the extinction contour belonging to the basal plane of the martensite. The lower the M_s temperature, the more pronounced is the mottling in the martensite. Fig. 10 shows the contrast effect in Cu-Zn-Al martensite, where the mottling appears only along the extinction contour belonging to the basal plane, which is the prominent curving contour. As can be seen from this same figure, the other extinction contours are not affected by mottling. Many of the dislocations present in the supersaturated β-phase

Figure 8 Retained β-phase in a Ag-39.1% Zn alloy pulse-heated to 348°C to form some Widmanstätten alpha-phase, then quenched. The α-phase shows none of the mottled contrast evident in the surrounding phase.

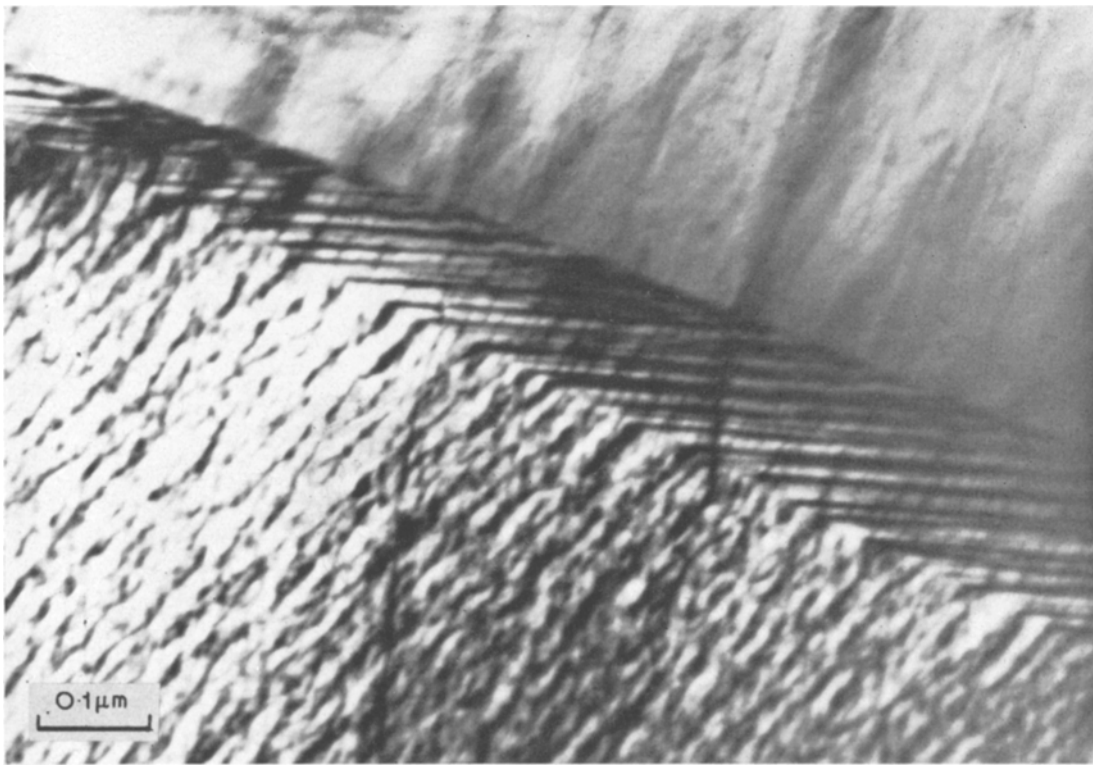

Figure 9 β-phase in a Cu-Zn alloy partially transformed to martensite (above) on quenching. The boundary between martensite and the beta-phase shows an association of linear features with contrast in the β-phase. The lack of contrast in the martensite is the result of the chosen orientation.

show a wavy configuration (Fig. 11). A careful examination of a tilt series shows that this wavy configuration is associated with the mottled areas. The density of the mottling does not change as the foil thickness changes, indicating that an increase in the amount of "interior" material does not add to the observed contrast in the foil. The constancy of this parameter is the best evidence for a surface condition leading to the mottled contrast effect. In the next section, this surface phenomenon will be discussed in more detail.

4.2. Surface rippling

The mottling shown in the micrographs of the previous section is due to surface rippling. Surface rippling or surface etch-pitting occurs frequently during electropolishing of metals and alloys. For example, a surface structure due to electropolishing even of pure Al has been reported by Welsh [22]. The fact that the surface is not smooth or free from pitting will of course influence the observed microstructure in transmission electron microscopy [23].

Surface rippling can be easily proved if the bulk material contains some planar boundaries such as twins, plates, etc. If the surface is perfectly flat, the intersection of a planar boundary with the foil surface will be a straight line and so will be the projection of this line on the fluorescent screen of the microscope. It is known that the α_m massive transformation product formed in certain β-brass type alloys typically contains thin twins. Such twins are shown in Fig. 12 for α_m-phase in a Cu-Zn alloy. The orientation of the thin foil in this case was such that only the microtwins were in the diffraction condition. From Fig. 12 it can be seen that the intersection of the twin with the surface is not a straight line but a wavy one, proving the surface rippling. Fig. 12b shows that as the twins become thicker, the mottled contrast can be seen in the areas where the twin boundaries do not overlap.

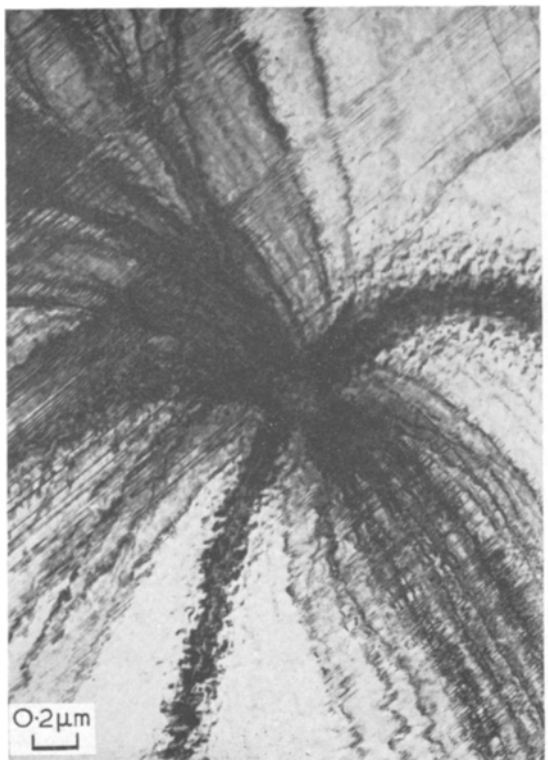

Figure 10 Mottling effects evident near the basal plane contour of martensite in a Cu-Zn-Al alloy. The prominent basal plane contour curves from bottom centre to right centre.

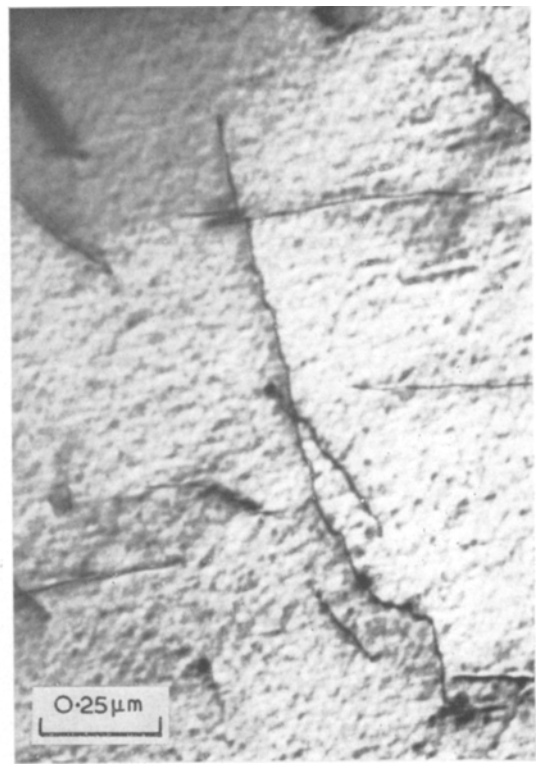

Figure 11 Wavy configuration of dislocations in a supersaturated Cu-Zn phase alloy.

Fig. 13 shows a similar waviness for stacking-fault fringes in the Ag-Cd α_m phase.

The effect of surface rippling on the diffraction contrast encountered in an electron transmission microstructure has been treated theoretically by Ashby and Brown [24]. They treat surface pits as inclusions, with these inclusions or holes having an extinction distance $\xi_g = \infty$. They show that in thin crystals, small changes in thickness of the crystal will be detected at locations where the intensity varies rapidly with thickness, that is, at locations where $S_g = 0$ and $t/\xi_g = 1/4, 3/4, 5/4$, etc. This means that the contrast will be at its maximum close to extinction contours, as shown by Fig. 14. This figure and all of the others presented thus far show mottled contrast that is compatible with the existence of surface rippling. Therefore, we conclude that the anomalous contrast effect observed here in supersaturated β- and α_m-phases, and denoted generally as "mottled structure" by various authors, is due at least in part to surface rippling. The maximum visibility is caused by structure factor contrast, because the structure factor F enters the intensity equation of Ashby and Brown [24] as the extinction distance $\xi_g = \pi V \cos\theta_g / F\lambda$. As already emphasized, the contrast effects due to electropolishing are a feature commonly observed in thin foils of various pure metals and alloys. However, the mottling in various β-brass type alloys has not been recognized as due to surface rippling because the effect is more pronounced, does not change with changing polishing conditions, and the associated diffraction patterns show anomalous streaking and extra intensity maxima. As will be shown in the following section, some form of precipitation is present in the β-phase. This precipitation causes surface rippling during electropolishing, giving rise to mottling effects. In addition, the small precipitates themselves will give rise to contrast effects. However, in order to study the contrast effects due only to the precipitates, one should start with a foil which has been electropolished *before* the precipitates are formed [29].

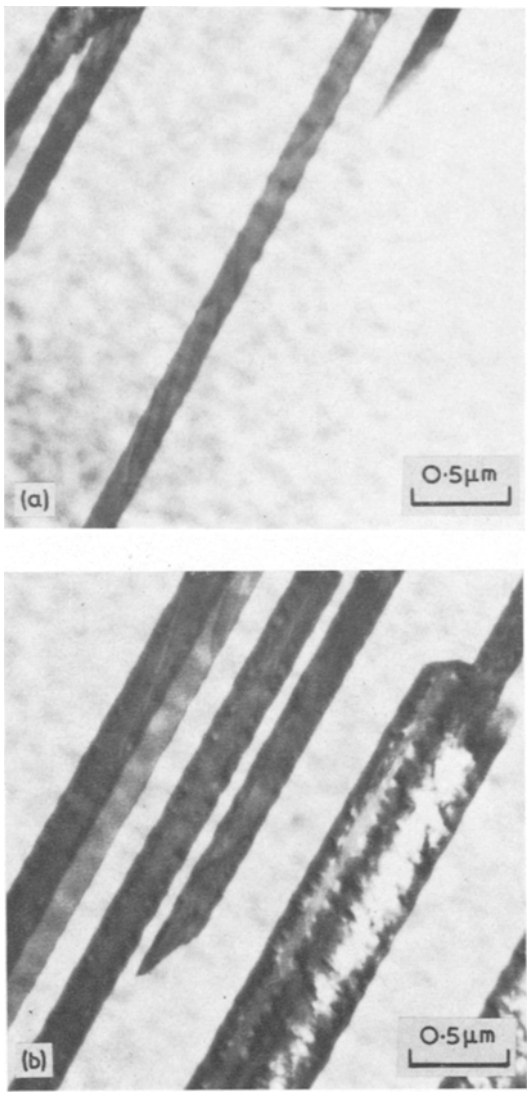

Figure 12 (a) Twins in Cu-Zn$_{\alpha_m}$ phase of a Cu-Zn alloy Wavy intersection with foil surface indicate surface rippling that is associated with fine scale precipitates. (b) Mottled contrast in twinned areas when the twins are thick enough and do not overlap.

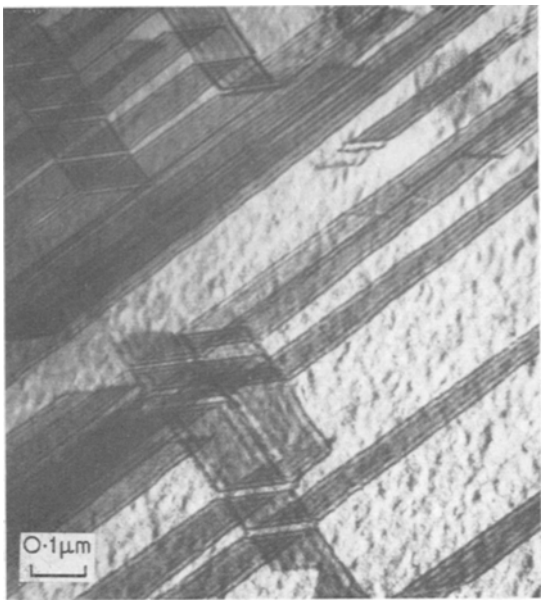

Figure 13 Waviness observable in stacking fault fringes of α_m-phase in a Ag-44.0% Cd alloy. They indicate fine scale periodic variations in the foil thickness.

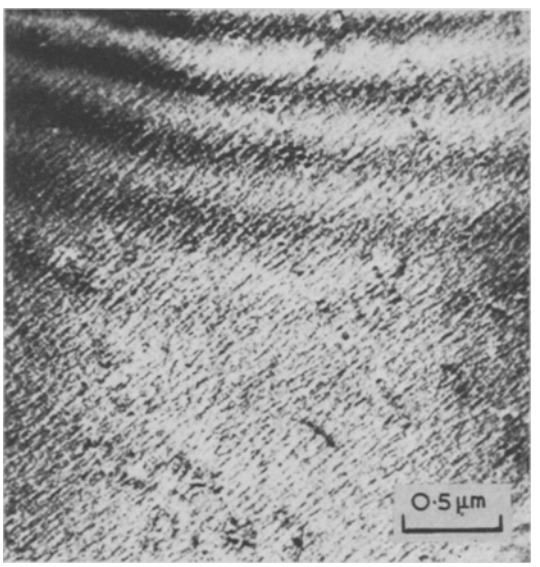

Figure 14 Cu-Zn β-phase foil. Contrast due to fine-scale thickness variations is greatest at extinction contours near the edge of the foil, where intensity varies most rapidly with thickness.

4.3. The electron diffraction patterns

The quenched supersaturated phases also show some anomalies in their diffraction patterns. Most of the information is obtained from diffraction patterns with the zone axis at or close to $\langle 100\rangle_\beta$, $\langle 110\rangle_\beta$, and $\langle 111\rangle_\beta$. Before an attempt is made to elaborate on the details of the reciprocal lattice of the quenched supersaturated β-phases, the diffraction patterns from the above-mentioned prominent zones will be discussed.

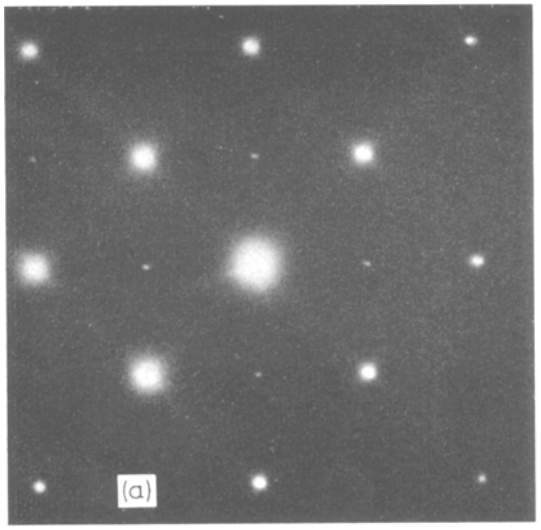

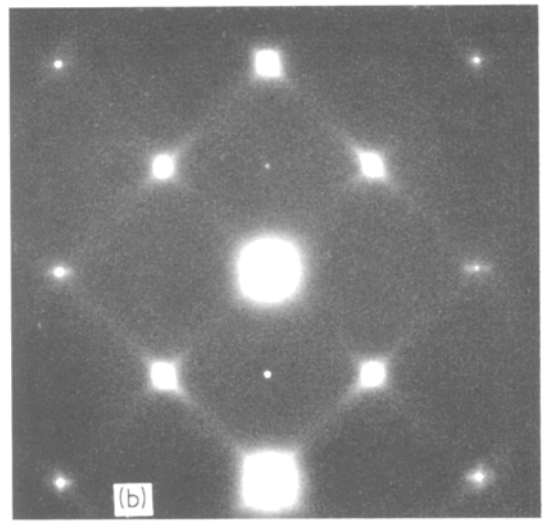

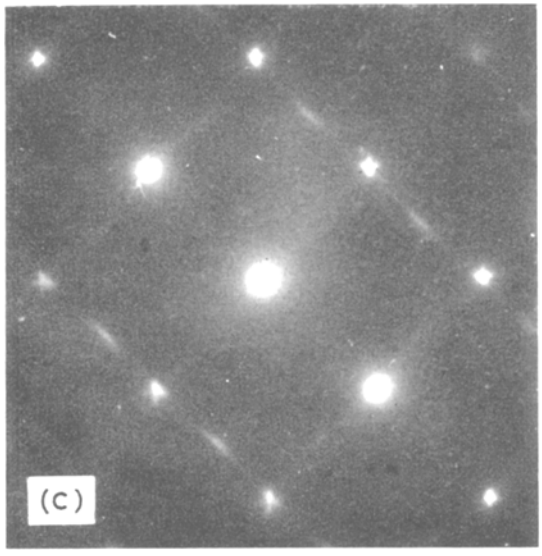

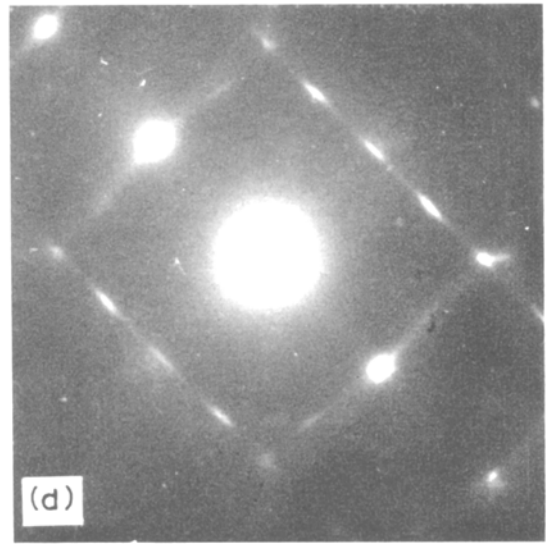

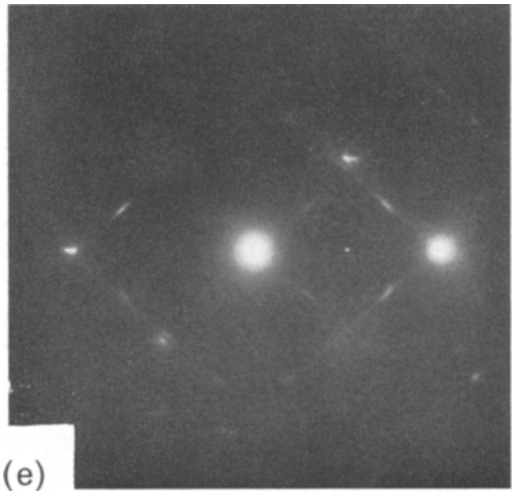

Figure 15 $\langle 100\rangle_\beta$-zone electron diffraction patterns. (a) Zone axis exactly along $\langle 100\rangle_\beta$ shows $\{001\}$-type superlattice spots of ordered supersaturated β-phase and streaks in [011] and $[0\bar{1}1]$ directions. (b) When orientation of (a) is slightly rotated around the [001] axis, satellites to main spots appear in $(010)_\beta$ and $(001)_\beta$ planes. (c) Orientation of (a) slightly rotated around the $[011]_\beta$ axis to reveal supplementary spots. (d) Orientation of (a) rotated further around $[011]_\beta$ than in (c). (e) Orientation of (a) rotated much further around $[011]_\beta$ than in (c) or (d).

4.3.1. $\langle 100\rangle_\beta$-zone electron diffraction patterns

The Figs. 15a, b, c, d and e are various electron diffraction patterns in which the zone axis is at or near to $\langle 100\rangle_\beta$. Fig. 15a shows a pattern with the

zone axis exactly along $\langle 100\rangle_\beta$, taken from the Cu-Zn β-phase. This diffraction pattern shows the $\{001\}_\beta$-type superlattice spots of the ordered supersaturated β-phase. Streaks are visible in the [0 1 1] and [0 $\bar{1}$ 1] directions. A careful examination of this diffraction pattern shows that the streaks contain weak intensity maxima, which are elongated in the streaking directions and are located around $\{0\frac{1}{2}\frac{1}{2}\}$. It is a common feature that the intensity of the maxima in one direction (e.g. [0 $\bar{1}$ 1]) is more intense than in the other direction (e.g. [0 1 1]). This suggests that the supersaturated β-phase contains areas which no longer have cubic symmetry. If the foil is slightly rotated around the $[001]_\beta$ axis, an electron diffraction pattern such as that shown in Fig. 15b is obtained. Around each main spot satellites appear lying in the $(010)_\beta$ and $(001)_\beta$ planes. If the foil is slightly rotated around the $[0\,1\,1]_\beta$ axis, diffraction patterns such as shown in Figs. 15c and d are obtained. The supplementary spots around and in between the matrix spots are clearly visible. It is also visible from Fig. 15d that the elongated spots do not lie exactly along the streaks. When the foil is tilted much more around $[0\,1\,1]_\beta$, Fig. 15e is obtained. It must be pointed out that in all of these $(001)_\beta$ patterns, the superlattice spots are not accompanied by any streaking or by satellite spots.

From the shape and behaviour during tilting of the elongated supplementary spots, which are shown in Fig. 15d for example as curved streaks, it may be concluded that the reciprocal lattice consists of interlacing relplanes; this means that the supersaturated β-phases contain chains of atoms whose positions deviate slightly from the ideal bcc atomic position. Alternatively the interpretation of the reciprocal lattice is consistent with needle-shaped precipitates.

Part of the reciprocal lattice can now be constructed using the foregoing electron diffraction patterns. Fig. 16a shows the $\{100\}_\beta$ reciprocal lattice plane and Fig. 16b shows a reciprocal lattice plane *close* to the $\{100\}_\beta$ orientation (the thin foil being rotated around the $\langle 001\rangle$-axis). The supplementary spots located at $\{0\frac{1}{2}\frac{1}{2}\}$ (Fig. 16a) are divided into two groups because the spots of group 1 do not always appear with the same intensity as the spots of group 2. The satellite spots visible around the main spots (Fig. 16b) are due to the intersection of the streaking lying along other $\langle 1\,1\,0\rangle$-directions, and cannot (because of symmetry reasons) be due to relpoints associated

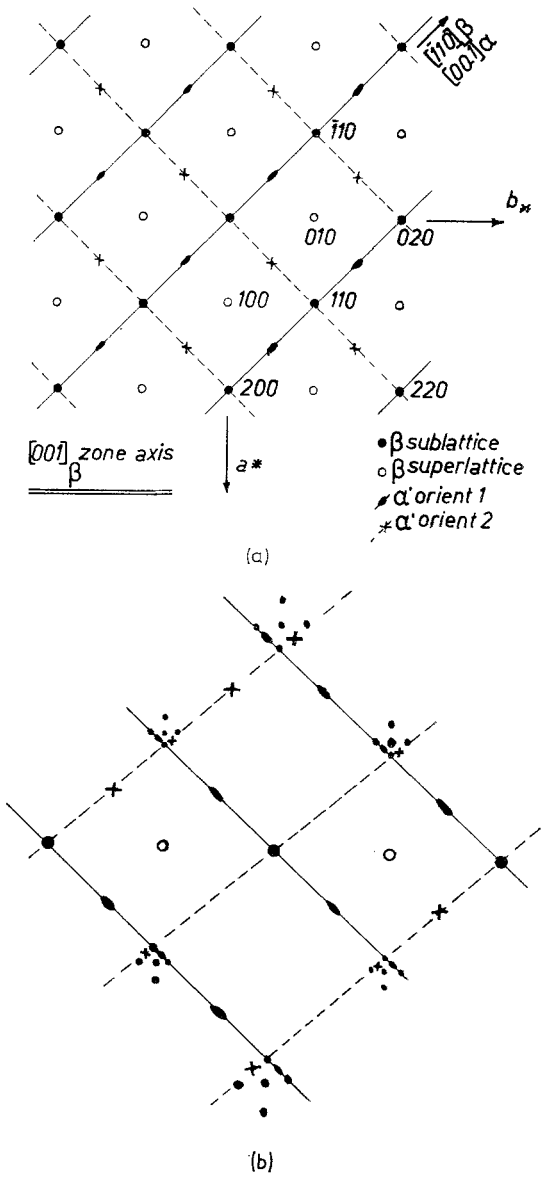

Figure 16 (a) Representation of a $\{100\}_\beta$ reciprocal lattice plane. (b) Reciprocal lattice plane close to $\{100\}_\beta$ (after slight rotation around $[001]_\beta$ axis), based on diffraction patterns such as those presented in Fig. 15.

with a precipitate. Examining closely some of the diffraction patterns (e.g. Fig. 14e) additional satellite spots could be drawn which are to be associated with those located at $\{0\frac{1}{2}\frac{1}{2}\}$. Fig. 17 shows that $\langle 100\rangle_{\alpha_m}$ diffraction patterns have similar features to those of the β-phase. Precipitates in the α_m-phases will be discussed in more detail in a later section.

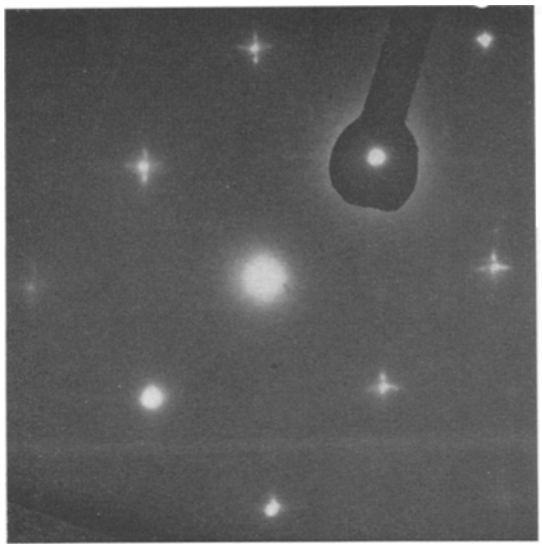

Figure 17 A $\langle 100 \rangle_{\alpha_m}$ diffraction pattern, showing similar features (satellites and streaks) to those observed in β-phases.

4.3.2. $\langle 111 \rangle_\beta$-zone electron diffraction patterns

Fig. 18a shows a typical $\langle 111 \rangle_\beta$ electron diffraction pattern, from the supersaturated β-Ag-Cd phase. This diffraction pattern shows streaking in all three $\langle 110 \rangle_\beta$- type directions, the streaking being more pronounced in one of these, the $[10\bar{1}]$ direction. Fig. 18c gives the interpretation of this diffraction pattern. If the foil is observed in an orientation close to $\langle 111 \rangle$, a pattern as illustrated in Fig. 18b is frequently found, wherein the maxima of the hcp phase are clearly visible. Fig. 19 shows the typical microstructure corresponding to a $\langle 111 \rangle_\beta$ foil orientation.

The reciprocal lattice can now be constructed in more detail. Fig. 20 gives three-dimensionally the positions of the reciprocal lattice of the β-phase, revealing the $\langle 100 \rangle$ and $\langle 111 \rangle$ diffraction patterns together with the positions of some of the additional spots. An analysis of the additional spots shows that the β-phase contains precipitates with a structure close to hcp. The orientation of this hexagonal phase with respect to the β-phase is close to $(110)_\beta // (0001)_{hex}$ and $|\bar{1}11|_\beta // |11\bar{2}0|_{hex}$. The same phase has recently

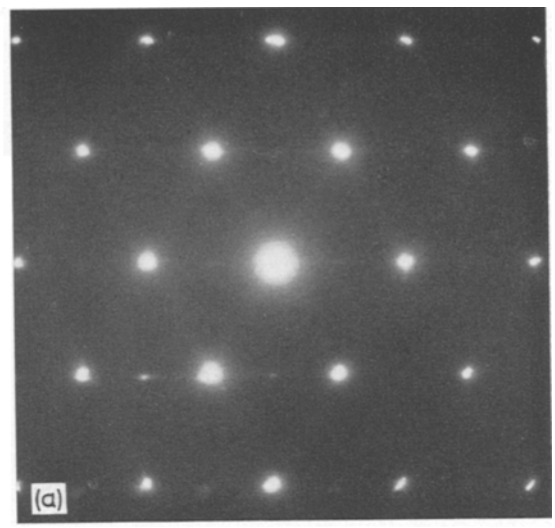

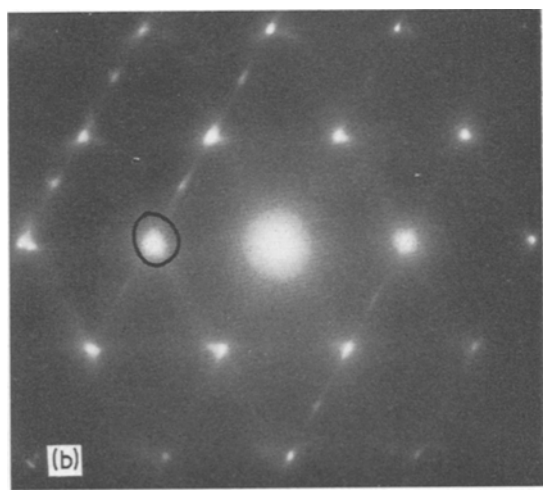

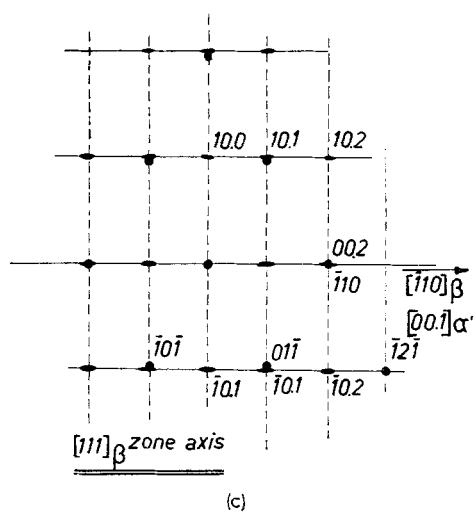

(c)

Figure 18

Figure 18 $\langle 111 \rangle_\beta$-zone electron diffraction patterns. (a) Exactly along $\langle 111 \rangle$, showing streaking in 3 $\langle 110 \rangle_\beta$ type directions. (b) Maxima corresponding to a close-packed hexagonal phase clearly visible in one set of streaks. (c) indexing of patterns of (a) and (b).

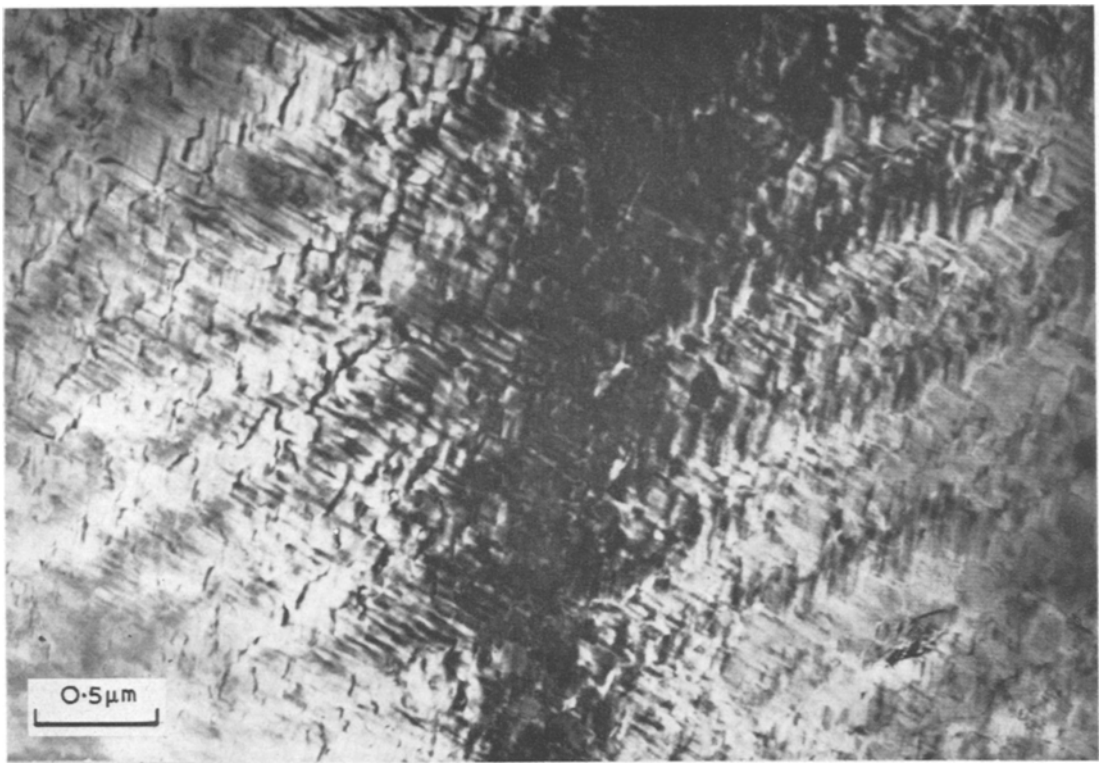

Figure 19 Typical β-phase contrast in a Ag-44.0% Cd foil oriented close to the $\langle 111 \rangle_\beta$ axis.

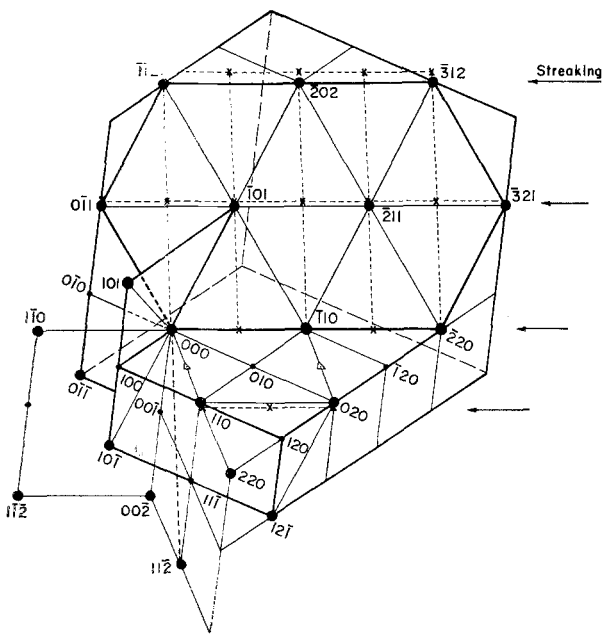

Figure 20 A three-dimensional representation of reciprocal lattice of quenched supersaturated β-phases, showing $\{100\}_\beta$ and $\{111\}_\beta$ sections, as well as the positions of additional spots.

been found and studied in much more detail [31, 32]. DeBondt and Deruyttère [32] obtained the hexagonal phase, called α', in Cu-Sn alloys by bainitic reaction. According to Vandermeulen [31], the same α'-phase occurs in the quenched β- and γ-CuSn phase on a much finer scale. Our results and observations are in accordance with this suggestion.

The contrast effects we observed in the microstructure of the different supersaturated β-phase may thus be correlated with these precipitates. Flewitt [25] has shown that the bainite formation in β-CuZn occurs as rods and that different rods are found as groups. Similarly, Tas and Delaey [30] showed that during the formation of martensite, in each group of the martensitic transformation products, the differently oriented plates or rods are arranged in such a way that the total deformation is zero, each group forming a self-accommodating system. We believe that this phenomenon most likely also accompanies the formation of the hexagonal phases in our alloys. Examining carefully the position of the supplementary spots and the streaking going through

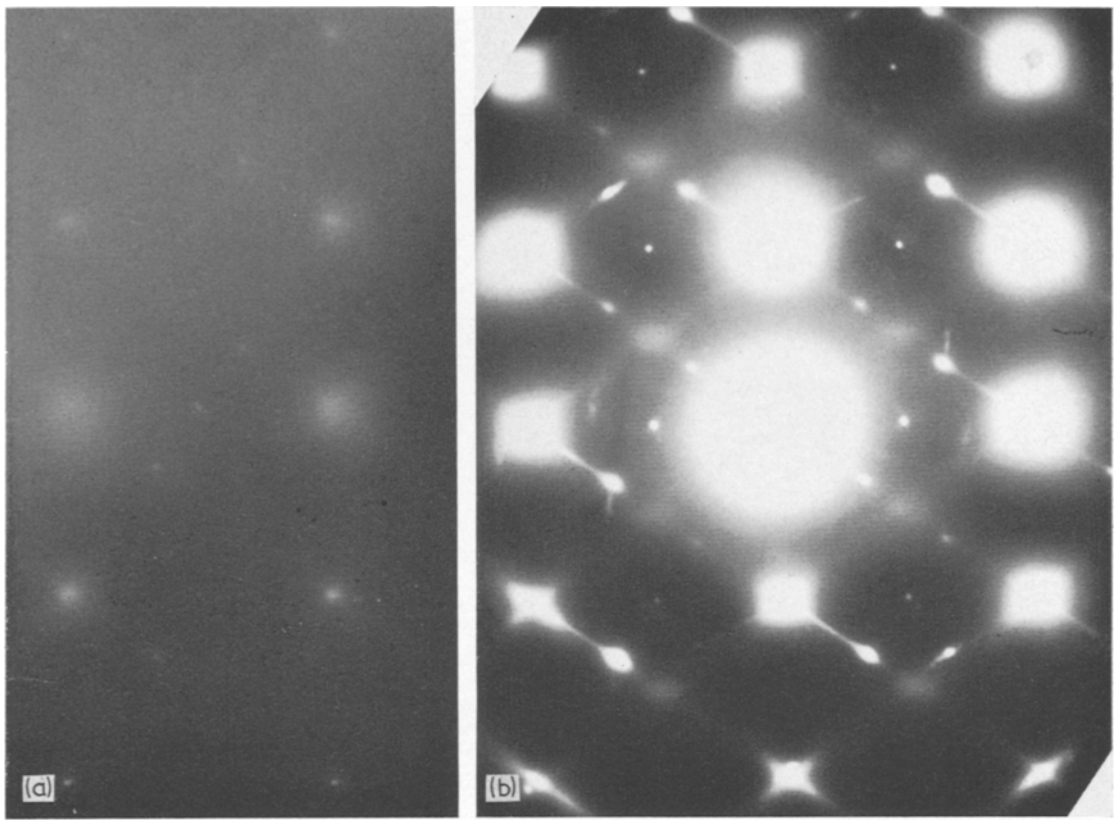

Figure 21 $\langle 110\rangle_\beta$-zone electron diffraction patterns. Additional spots are seen which can be identified with the hexagonal ω-phase. These are seen in both the supersaturated (quenched) β-phase (a), and the stable β-phase (b). The α' phase is seen only in the former case.

them we come to the conclusion that we are dealing with faulted close-packed structures.

4.3.3. $\langle 110\rangle_\beta$-zone electron diffraction patterns

On tilting the specimen to orientations near $\langle 110\rangle_\beta$ some further unidentified spots appear on the electron diffraction patterns. After examining series of diffraction patterns, the unidentified spots can be identified with the ω-phase (Fig. 21a). The structure of this ω-phase is to be compared with the ω-phase, which occurs in some Ti-alloys. The reciprocal lattice and hence the diffraction patterns differ somewhat from those of the ω-phase in the Ti-alloys, because we are dealing with two different atoms. The small crystallographic differences between the two types of ω-phase have been dealt with extensively by Vandermeulen [31].

The spots belonging to the ω-phase also appear in electron diffraction patterns of the stable β-phase, whereas the α'-phase does not appear in these alloys (Fig. 21b). From the $\langle 110\rangle_\beta$-zone electron diffraction patterns it may be concluded that the supersaturated quenched β-phases contain mostly very fine dispersed precipitates from two phases: the nearly hexagonal bainitic α'-phase and the hexagonal ω-phase. The ω-phase is characterized by the following orientation relationship $(111)\beta // (0001)_\omega$ and $|\bar{1}\bar{1}0|_\beta // |2\bar{1}\bar{1}0|_\omega$. Fig. 22 schematically describes the features of the $\langle 110\rangle_\beta$ diffraction patterns.

4.3.4. Continuous streaking in the electron diffraction patterns

Beside the above-discussed supplementary spots in the electron diffraction patterns, streaking is visible on nearly all the diffraction patterns. Tilting experiments have shown that the reciprocal lattice contains diffuse broad relrods and rel-

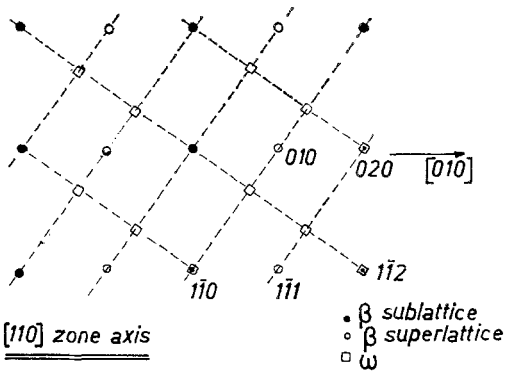

Figure 22 A schematic representation of a $\langle 110 \rangle_\beta$ diffraction pattern, locating beta and omega reflections.

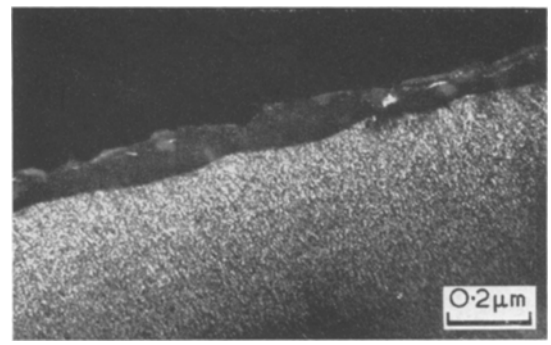

Figure 23 High resolution matrix dark field mode observation of a supersaturated β-phase in a Cu-Zn alloy.

planes (Fig. 18b). The diffuse streaking lies along all the $\langle 110 \rangle_\beta$-directions, the relplanes are lying along planes perpendicular to the $\{111\}_\beta$ planes. The streaking (relrods and relplanes) shows that in the β-phase, amplification of certain vibrational modes occurs in a given temperature range, reflecting the incipient instability of the bcc lattice. The more detailed nature of the vibrational modes and their general influence on the stabilization of the β-phase will be discussed elsewhere [33], where it will be shown that the amplification of certain vibrational modes, and the occurrence of the ω- and α'-transition forms constitute additional features that contribute to the overall mechanism of stabilization associated with the β-phases at different temperatures.

Clearly, at least in the β-brass type phases, the overriding stabilizing feature is the electron concentration, approximately 1.5 e/a. Once this condition is satisfied, the general stability and the shape of the phase field will depend on the temperature and on the nature of the solute and solvent atoms present, their proportion, chemical affinity, size disparity, etc. The degree and the type of order, evident particularly at low temperatures, will depend on all these factors. In brasses formed with two-valent solutes the tendency towards CsCl-type of order is overwhelming; with three-valent solutes the less stable $FeAl_3$-type of order occurs. As the temperature is increased, contribution to stability from ordering diminishes while that from various vibrational modes of the lattice increases. It is in this region of intermediate temperature, therefore, that the β-phases appear to be particularly susceptible to developing specific vibrational states that enhance stability. Such states may take the form of enhanced vibrational modes that resemble TDS, or the more complex ω or α' transitional forms. The relationship between order, electronic features and the lattice structure in such forms is still far from clear.

5. The visibility of the precipitates

The α'- and ω-precipitates in supersaturated and equilibrium β-phase of the noble metal base alloys are visible in bright field images provided that the orientation of the foil is close to a prominent matrix zone. The use of high-resolution dark-field techniques as shown in Fig. 23 yields no further information, except that the visibility of the precipitates is maximum in the thinnest areas. The variation of visibility with foil thickness and orientation is governed by structure factor contrast, as explained by Ashby and Brown [24]. The contrast effects observed in the present case are enhanced by surface relief effects which are more pronounced in alloys exhibiting the α'-phase, whereas the contrast effects are less in equilibrium alloys containing only the ω-phase (Fig. 24).

The precipitates occurring in the massive α_m-phase is in certain cases, as e.g. α_m-AgCd (Fig. 25), clearly recognizable as consisting of relatively large plates. Part of the contrast effects are to be explained by Moiré effects, the plates being parallel with the $\{111\}_{\alpha_m}$-planes. The electron diffraction patterns show clearly that, in the case of Ag-Cd, we are dealing with a hexagonal close packed plane. It is believed that in this particular case this phase has to be identified with the ζ-AgCd phase. This example shows that, beside the above-discussed α'- and ω-phases, other phases, which are characteristic only for the particular alloy, may occur in the

Figure 24 Contrast as observed in a stable β-phase Cu-48.5% Zn alloy containing only ω-phase. This contrast is less pronounced than in a supersaturated β-phase also containing α' component.

quenched α- and β-phases. Similar Moiré fringe patterns are also associated with precipitates in the β-phase (Fig. 26). Fig. 26 is taken from a Ag-Zn specimen pulse-heated to form α_w and then quenched; a featureless α_w needle is seen in the centre of the retained mottled β-phase matrix. Fig. 27 shows the mottled β-phase matrix surrounding wing-shaped bainite plates in Ag-Cd (note that only one of the two plates making up the centre wing is in contrast). Some mottling is also observed in the bainite. It is also believed that some of the supplementary intensity maxima observed in CuSn by Warlimont [15] are due to a phase particular to CuSn [31].

6. The stability of β-phase alloys

The stability of the beta brass-type phase in noble-metal alloys has been often described in terms of entropy stabilization at high temperatures, while the bcc structure is known to be "mechanically unstable" to certain types of elastic deformation (to new structures) at low temperatures. The parameter classically examined is the anisotropy ratio, A, expressed in terms of elastic shear coefficients $A = C_{44}/\frac{1}{2}(C_{11}-C_{12})$.

Figure 25 Precipitates in the massive α_m-phase of a Ag-44.5% Cd alloy. The precipitates are in plate form parallel to $\{111\}_{\alpha_m}$ planes. This HCP phase is most likely the equilibrium ξ-phase present in the Ag-Cd system.

In this expression, the term C_{44} refers physically to a shear across the (100) plane in an arbitrary

Figure 26 Moiré fringe patterns associated with large metastable precipitates in the supersaturated β-phase of a Ag-39.1% Zn alloy.

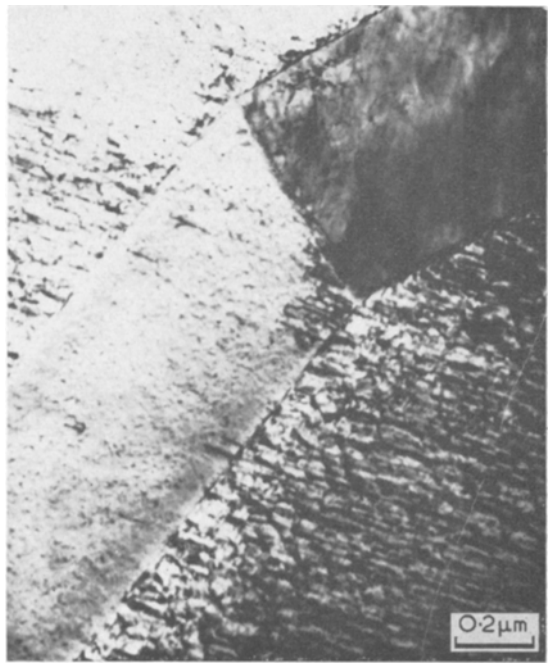

Figure 27 Mottled contrast in the β-phase of a Ag-44.8% Cd alloy which has developed bainite during cooling. Only one of the bainite plates making up the typical cant-winged feature is in contrast.

direction, while the term $\frac{1}{2}(C_{11} - C_{12})$ refers to a shear across the (110) plane in the $|1\bar{1}0|$ direction. As described by Zener [34], a high value of this ratio, as in the case of beta-phases, therefore indicates that the bcc structure is unstable with respect to a (110) $|1\bar{1}0|$ shear which will lower the energy of the system by the maximum amount. This instability is therefore often manifested by a martensitic transformation of the bcc structure via this very shear mode, when quenched. The anisotropy ratio can also be approximately related to a ratio of the elastic moduli $E\langle 111\rangle/E\langle 100\rangle$. A high or low value of the ratio in this case leads to the concept of "soft" $\langle 100\rangle$ or $\langle 111\rangle$ directions respectively.

It has not been fully appreciated until recently that electronic entropy terms can play an equally important role in phase stability. Although it seems rather apparent that changes in bonding character must accompany structural changes, electronic transitions in the atoms of elements or alloys have not often been cited as the cause of phase changes. An exception has arisen in recent studies of transitions observed in the metastable beta phase of bcc transition-metal alloys [26]. The best known of these has been designated the "omega" transition, which occurs in numerous alloys of Ti group elements with transition metals. The instability of the bcc phase in this case again manifests itself on cooling below a critical temperature, not by a martensitic shear transformation, but by the homogeneous operation of certain lattice vibration modes throughout the bcc structure. The particular phonon modes are unique and can be related to electronic changes in the atoms of the alloys which cause the atoms of the unit cell to fluctuate toward new spatial arrangements (angles and distances) characterizing a new bonding nature. In the case of the omega transition, this can be most simply described as the introduction of more covalent character into the bond hybrids as the structure changes from beta-phase to omega-phase. Another example of this type of general lattice instability characterized by vibration waves

occurs in the CsCl (B2) lattice of equiatomic TiNi alloys when cooled below a critical temperature [27]. In this case, the phonon range is climaxed by a shear transformation of the (1 1 2) ⟨1 1 1⟩ type, which is believed to be intimately related to the atom motions involved in the preceding unique lattice modes.

The point of the above discussion is to establish that beta-phase instability at low temperatures can be demonstrated in many ways that cannot be classified into conventional phase-transformation categories. Even the mechanical stability arguments such as put forth initially by Zener, have little usefulness in predicting the way in which beta-phases will change structure when electronic changes in the atoms are involved. In this case, it is pair-wise atomic interactions that become important, and lattice vibrations of very short wavelengths must be considered to be more significant than the long-wavelength elastic waves of macroscopic deformations considered in simple mechanical stability discussions. For example, the lattice instability in bcc transition metal alloys mentioned above involves the operation of transverse lattice vibrations of wavelengths on the order of the bcc unit cell size, usually polarized in ⟨1 1 1⟩ directions. This implies the co-ordinated movement of the close-packed ⟨1 1 1⟩ chains in the bcc structure with respect to each other, but does not at all follow from consideration of the effects of macroscopic shears on the energy of crystals.

In the case of the homogeneous lattice instability described above for the bcc-omega transition and the pre-martensitic transition in B2 TiNi, experimental evidence for both effects is generally similar to the observations made here in supersaturated noble metal beta-phases. Beta-phase mottling in transmission images and diffuse diffraction scattering in certain temperature ranges are typical features in both cases. In searching for the fundamental origin of a particular mode of beta-phase instability, there are many criteria that can be selected in order to base an argument. For example, the omega instability of bcc transition-metal alloys has been related to electronic changes in the individual atoms as a function of temperature, while beta-brass transformations at low temperatures have historically been more closely connected to mechanical instability that culminates in collapse of the structure by martensitic shear. However, the situation in the case of supersaturated beta-phases, such as those examined in the present study, is believed to be not so simply described, and may have a significant casual similarity to the type of lattice instability exhibited by the transition metal alloys. The diffuse diffraction effects shown by some alloys, such as Cu-Sn in the single-phase beta field [13] are quite similar to the scattering effects expected from short-wavelength lattice waves.

From our observations made on the structure and microstructure of quenched β-brass type alloys the following conclusions with regard to the stabilization of the quenched β-brass type alloys can be made:

1. Contrast effects in quenched β-brass phases can be attributed to a combination of thickness contrast (surface rippling) structure factor contrast, and Moiré fringe effects.

2. Surface rippling, when observed in electropolished β-brass foils is associated with underlying fine-scale metastable precipitation in the β-phase.

3. Quenched supersaturated β-phases precipitate the metastable α' and ω phases, whereas the equilibrium-aged beta-phase is found to contain only the ω-phase.

4. Diffuse intensity-streaking in diffraction patterns of metastable beta-phases reflects the operation of enhanced vibration modes within the beta-phase, or the dynamic nature of the transition structures.

5. Both α' and ω formation can be associated with details of the bcc phonon spectrum in certain temperature ranges. These details are left to a later paper [33].

6. Depending upon the alloy system, the subsequent formation of other fine-scale precipitates can, if further shear or short-range diffusional processes are possible, contribute to a greater stability of the assembly of phases, which is macroscopically represented by the β-phase.

Acknowledgements

The authors wish to express their thanks to Dr W. Vandermeulen and Dr J. Van Paemel for helpful and stimulating discussions. They are grateful to Dr R. DeRidder of RUCA, Antwerp and to Professor S. Amelinckx for taking and commenting on the optical diffractogram shown in Fig. 5.

This work was made possible in part by a grant from the Belgian National Fonds voor Wetenschappelijk Onderzoek (including travel support for Dr L. Delaey's visit to the USA) and by a grant from the US Army Research Office,

Durham, North Carolina, both of which are gratefully acknowledged.

References

1. H. WARLIMONT and L. DELAEY, *Prog. Mater. Sci.* (to be published).
2. R. F. HEHEMANN, "The Bainite Transformation", in "Phase Transformations" (ASM Metals Park, Ohio, 1970) p. 397.
3. H. M. CLARK and C. M. WAYMAN, "Surface Relief Effects in Solid-State Phase Transformations" in "Phase Transformations" (ASM, Metals Park, Ohio, 1970) p. 59.
4. R. D. GARWOOD, Special Report No. 93 (The Iron and Steel Institute, London, 1965) p. 90.
5. T. B. MASSALSKI, "Massive Transformations", in "Phase Transformations" (ASM, Metals Park, Ohio, 1970) p. 433.
6. S. SATO and K. TAKEZAWA, *Trans. JIM* **9** (Supplement) (1968) 925.
7. H. POPS and M. AHLERS, in "The Mechanism of Phase Transformations in Crystalline Solids", Institute of Metals Monograph No. 33 (London 1969) p. 197.
8. E. HORNBOGEN and H. WARLIMONT, *Acta Metallurgica* **15** (1967) 943.
9. E. HORNBOGEN, *Z. Metallk.* **50** (1959) 70.
10. S. T. SCHEIRER, Ph.D. Thesis, Case Western Reserve University, 1969.
11. J. A. MALCOLM and G. R. PURDY, *Trans. AIME* **239** (1967) 1391.
12. E. B. HAWBOLT and T. B. MASSALSKI, *Met. Trans.* **1** (1970) 2315.
13. Z. NISHIYAMA, H. MORIKAWA, and K. SHIMIZU, *Jap. J. Appl. Phys.* **6** (1967) 815.
14. H. MORIKAWA, K. SHIMIZU, and Z. NISHIYAMA, *Trans. Jap. Inst. Metals* **8** (1967) 145.
15. H. WARLIMONT, Proc. Sixth International Congress for Electron Microscopy, Kyoto (1966) p. 437.
16. L. E. TANNER, *Phil. Mag.* **14** (1966) 111.
17. W. K. ARMITAGE, P. M. KELLY, and J. NUTTING, Proc. Fifth International Congress for Electron Microscopy, 1962, p. K-4.
18. K. OTSUKA and K. SHIMIZU, *Jap. J. Appl. Phys.* **8** (1969) 1196.
19. A. J. PERKINS and T. B. MASSALSKI, *Met. Trans.* **2** (1971) 2701.
20. D. HULL, *Phil. Mag.* **7** (1962) 537.
21. J. D. AYERS and T. B. MASSALSKI, *Met. Trans.* **3** (1972) 261.
22. N. C. WELSH, *J. Inst. Metals*, **85** (1956-57) 129.
23. P. B. HIRSCH *et al*, "Electron Microscopy of Thin Crystals" (Butterworths, London, 1965) p. 50.
24. M. F. ASHBY and L. M. BROWN, *Phil. Mag.* **8** (1963) 1649.
25. P. E. FLEWITT, *Scripta Met.* **2** (1968) 161.
26. A. J. PERKINS, Ph.D. Thesis, Case Western Reserve University, 1969.
27. A. J. PERKINS, G. SANDROCK, and R. F. HEHEMANN, *Met. Trans.* **2** (1971) 2769.
28. D. A. KARLYN, J. W. CAHN, and M. COHEN, *Trans. Met. Soc. AIME*, **245** (1969) 197.
29. R. CADORET and P. DELAVIGNETTE, *Phys. Stat. Sol.* **32** (1969) 853.
30. H. TAS and L. DELAEY, to be published.
31. W. VANDERMEULEN, Ph.D. Thesis, Leuven (1971).
32. M. DEBONDT and A. DERUYTTÈRE, *Acta Metallurgica*, **11** (1967) 993.
33. J. VAN PAEMEL, Engineer's Thesis, Leuven (1971),
34. C. ZENER, "Elasticity and Anelasticity of Metals" (University of Chicago Press, 1948).

Received 14 February and accepted 21 March 1972.